



**Universiteit
Leiden**
The Netherlands

Pressure-volume loop validation of TAPSE/PASP for right ventricular arterial coupling in heart failure with pulmonary hypertension

Schmeisser, A.; Rauwolf, T.; Groscheck, T.; Kropf, S.; Luani, B.; Tanev, I.; ... ; Braun-Dullaes, R.C.

Citation

Schmeisser, A., Rauwolf, T., Groscheck, T., Kropf, S., Luani, B., Tanev, I., ... Braun-Dullaes, R. C. (2021). Pressure-volume loop validation of TAPSE/PASP for right ventricular arterial coupling in heart failure with pulmonary hypertension. *European Heart Journal - Cardiovascular Imaging*, 22(2), 168-176. doi:10.1093/ehjci/jeaa285

Version: Publisher's Version

License: [Creative Commons CC BY 4.0 license](https://creativecommons.org/licenses/by/4.0/)

Downloaded from: <https://hdl.handle.net/1887/3279635>

Note: To cite this publication please use the final published version (if applicable).

Pressure–volume loop validation of TAPSE/PASP for right ventricular arterial coupling in heart failure with pulmonary hypertension

Alexander Schmeisser^{1†}, Thomas Rauwolf^{1*†}, Thomas Groscheck¹,
Siegfried Kropf², Blerim Luani¹, Ivan Tanev¹, Michael Hansen¹,
Saskia Meißler¹, Paul Steendijk³, and Ruediger C. Braun-Dullaes¹

¹Division of Cardiology and Angiology, Department of Internal Medicine, Magdeburg University, Leipziger Str. 44, D-39120 Magdeburg, Germany; ²Institute of Biometry and Medical Informatics, Magdeburg University, D-39120 Magdeburg, Germany; and ³Department of Cardiology, Leiden University Medical Center, 2333 ZA Leiden, The Netherlands

Received 4 July 2020; editorial decision 28 September 2020; accepted 5 October 2020; online publish-ahead-of-print 9 November 2020

Aims

The aim of this study was to validate the tricuspid annular plane systolic excursion/systolic pulmonary artery (PA) pressure (TAPSE/PASP) ratio with the invasive pressure–volume (PV) loop-derived end-systolic right ventricular (RV) elastance/PA elastance (Ees/Ea) ratio in patients with heart failure with reduced ejection fraction (HFREF) and secondary pulmonary hypertension (PH).

Methods and results

The relationship of TAPSE and TAPSE/PASP with RV–PV loop (single-beat)-derived contractility Ees, afterload Ea, and Ees/Ea was assessed in 110 patients with HFREF with and without secondary PH. The results were compared with other surrogate parameters such as the fractional area change/PASP ratio. The association of the surrogates with all-cause mortality was evaluated. In patients with PH ($n = 74$, 67%), TAPSE significantly correlated with Ees ($r = 0.356$), inverse with Ea ($r = -0.514$) but was most closely associated with Ees/Ea ($r = 0.77$). Placing TAPSE in a ratio with PASP slightly reduced the relationship to Ees/Ea ($r = 0.71$) but was more closely related to the parameters of PA vascular load, diastolic RV function, and RV energetics. The area under the curve of TAPSE/PASP and TAPSE for discriminating overall survival in receiver operating characteristic analysis was not different ($P = 0.78$). Prognostic relevant cut-offs were 17 mm for TAPSE and 0.38 mm/mmHg for TAPSE/PASP. Both parameters in multivariate cox regression remained independently prognostically relevant.

Conclusion

TAPSE is an easily and reliably obtainable and valid surrogate parameter for RV–PA coupling in PH due to HFREF. Putting TAPSE into a ratio with PASP did not further improve the coupling information or prognostic assessment.

Trial Identifier

DRKS—German Clinical Trials Register (DRKS00011133; https://www.drks.de/drks_web/navigate.do?navigationId=trial.HTML&TRIAL_ID=DRKS00011133).

Keywords

right ventricle–pulmonary arterial coupling • TAPSE • TAPSE/PASP • pressure–volume loops

Introduction

The functional and haemodynamic sequelae of secondary pulmonary hypertension (PH) in heart failure with reduced ejection fraction (HFREF) are directly linked to the adaptive intrinsic contractility response of the right ventricle (RV) to the pulmonary vascular load

[RV–pulmonary arterial (PA) coupling].¹ The quantification of RV–PA coupling is complex, because it needs a measure that determines both intrinsic RV contractility and RV afterload simultaneously. One such approach was proposed by Sagawa² for left ventricular–systemic vascular interaction based on invasive pressure–volume (PV) loops. Using this method, load-independent contractility coincides with

* Corresponding author. Tel: +49 (391) 67 13203/15206; Fax: +49 (391) 67 15211. E-mail: Thomas.Rauwolf@med.ovgu.de

†These authors contributed equally to this work.

Published on behalf of the European Society of Cardiology. All rights reserved. © The Author(s) 2020. For permissions, please email: journals.permissions@oup.com.

end-systolic elastance (Ees) and this way equals to the slope of the end-systolic pressure (ESP) to end-systolic volume relationship.^{2,3} Effective pulmonary arterial elastance (Ea), a lumped parameter of afterload, is defined by an ESP vs. stroke volume (SV) ratio.⁴ Because Ea is determined using the same units as Ees, the ratio of Ees to Ea becomes a unitless value that encapsulates a suitable quantitative assessment of RV–PA coupling.⁵

However, measuring Ees and Ea via PV loops is invasive and technically demanding. Therefore, simple non- or semi-invasive surrogates are being sought. One of the most promising surrogates with prognostic relevance is the Doppler echocardiographic determination of the tricuspid annular plane systolic excursion (TAPSE)/systolic PA pressure (PASP) ratio. The TAPSE/PASP ratio was originally described as an index of *in vivo* RV shortening in the longitudinal axis vs. developed force (length–force relationship) in patients with left heart failure.⁶ Recently, Tello *et al.*⁷ published first data about validation of the non-invasive TAPSE/PASP by the invasive PV loop-derived single-beat (SB) analysis. The TAPSE/PASP emerged as an independent predictor of invasive Ees/Ea in patients with pulmonary arterial hypertension and chronic thromboembolic PH. However, their results were not able to completely clarify the role of TAPSE/PASP as a straightforward surrogate of invasively measured Ees/Ea. The authors, for example, found no correlation of TAPSE/PASP to RV contractility Ees and the moderate correlation with Ees/Ea ($r=0.440$) was surprisingly not higher than to RV afterload (Ea, $r=-0.494$). In addition, their study contained no information on the relationship of TAPSE alone, independently of PASP. Furthermore, the applicability of the results by Tello *et al.*⁷ to patients with secondary PH due to HFREF remains controversial. The pathophysiology of RV failure in HFREF seems more complex, as more factors than afterload increase affect the RV contractility adaptation in this situation. The RV itself, for example, may be involved in the cardiomyopathic process of HFREF or the contractile left ventricle (LV) dysfunction compromises the systolic LV-to-RV myocardial crosstalk.⁸

We, therefore, assessed the relationship of TAPSE as a single parameter and in combination with PASP (TAPSE/PASP) with the SB PV loop-derived parameter of RV contractility (Ees), RV afterload (Ea), and RV–PA coupling (Ees/Ea) in patients with secondary PH due to HFREF. The same analysis was done with FAC and FAC/PASP. In addition, associations of TAPSE, FAC, and their ratio to PASP with prognosis were evaluated.

Methods

The Magdeburger CRT-responder trial was a prospective monocentric study of patients with standard CRT indications (NYHA II/III, LV ejection fraction $\leq 35\%$, and QRS ≥ 130 ms).⁹ The study was approved by the Institutional Review Board. All patients gave written informed consent. Within this exploratory study, we carried out a clinical examination program prior to implantation (Supplementary data online, Table S1).

This *post hoc* analysis is based on 110 included patients with baseline RV–PV loop and Swan-Ganz catheter measurement. All patients underwent echocardiography within 2 days before PV loop and Swan-Ganz catheter measurement. The clinical follow-up was performed every 6 months.

Echocardiography

Echocardiographic analysis was performed by two independent specialists using Xcelera and QLAB 8.1 (Phillips, The Netherlands). The forward SV, TAPSE, and FAC, including the systolic and end-diastolic area, the tricuspid regurgitation (TR) velocity, and the severity of TR were determined and/or quantified according to the current recommendations.^{10,11}

Left and right heart catheterization and RV–PV loop catheter

Left and right heart catheter measurements were performed as described previously.⁹ The trans-pulmonary gradient, the diastolic pressure gradient, and the pulmonary vascular resistance (PVR) were calculated using standard formulas. The PA compliance was determined as the ratio between the forward SV and the pulmonary pulse pressure. The secondary PH Group 2 was defined by a PAm_{mean} ≥ 25 mmHg and PCWP > 15 mmHg at rest. The isolated post-capillary pulmonary hypertension (IpcPH) was differentiated from combined post-capillary pulmonary hypertension (CpcPH) by PVR $< vs. \geq 3$ wood units.¹² A 7F RV–PV catheter (CD Leycom, The Netherlands) was positioned via the internal jugular vein for PV loop analysis. The RV haemodynamics and RV–pulmonary coupling were analysed by Circlab software (Leiden University, The Netherlands). The RV conductance data were calibrated as described previously.⁹ The slope factor alpha was determined by matching with the mean of the echovelocity time integral SV and cardiac output, and Fick-derived cardiac output, and parallel conductance was determined by hypertonic saline injections. The end-systolic PV relationship was determined by using SB approaches for load-independent systolic RV function.¹³ The latter was quantified by the slope (SB–Ees) and the volume intercept (RV volume at pressure of 25 mmHg, V25) of the end-systolic PV relationship. The RV afterload was determined by effective arterial elastance (SB–Ea, calculated as RV ESP/SV). Regarding the RV end-systolic point, we used the maximal RV pressure at minimum volume, which denotes the point of end-ejection, but not below RV dp/dt_{min} in case of true triangular PV loop curves without a demarked shoulder region. Ventricular pulmonary coupling was quantified as SB–Ees/Ea (Supplementary data online, Figure S1).

Statistics

All data and statistics are reported as mean \pm standard deviation for normally distributed data or as median and inter-quartile range (25–75%) for not normally distributed variables, respectively. Categorical data were summarized by percentages. Baseline characteristics were compared using the Wilcoxon rank sum test for continuous variables and the χ^2 test for categorical variables. Correlation analysis was used to analyse the relationship of TAPSE, TAPSE/PASP, FAC, and FAC/PASP with PV loop parameters and with the Swan-Ganz catheter-derived vascular. We used the test statistics published previously¹⁴ to compare the dependent Pearson and Spearman correlation coefficients. The receiver operating characteristic (ROC) curves were used to identify and compare the power of TAPSE vs. TAPSE/PASP and FAC vs. FAC/PASP to discriminate between surviving and non-surviving.¹⁵ The Kaplan–Meier method was used to estimate the all-cause mortality compared with log-rank test. Cox regression analysis was used for the analyses of predictors of mortality. Variables with $P < 0.1$ in univariate analyses perceived as clinically important and were included in two multivariate models. Differences with $P < 0.05$ were considered statistically significant. The multicollinearity was assessed. The Statistical Package for Social Sciences software (SPSS 24, IBM, USA) was used.

Results

Seventy-four (67%) patients with advanced HFREF presented with secondary PH (PAm_{ean} ≥25 mmHg). The baseline parameters are summarized in [Supplementary data](#) online, [Table S2A](#), divided according to the presence of secondary PH, combined, and isolated post-capillary PH (CpcPH and lpcPH) ([Supplementary data](#) online, [Table S2B](#)).

PV loop analysis of TAPSE vs. TAPSE/PASP in patients with secondary PH

TAPSE/PASP has been considered a surrogate of invasive PV loop-derived Ees/Ea based on the assumption that TAPSE estimates RV contractility and PASP estimates afterload.⁶ Actually, our data show that TAPSE only slightly correlated with intrinsic RV contractility Ees ($r=0.36$, $P<0.05$). However, the relationship of TAPSE to the coupling ratio Ees/Ea ($r=0.77$, $P<0.001$) was impressively closer (difference of correlations $P<0.001$). Placing TAPSE in ratio with PASP (TAPSE/PASP ratio) did not increase the association with Ees/Ea ($r=0.71$, $P<0.001$) (difference of correlations $P=0.056$) and was not associated with RV contractility Ees ([Figure 1](#) and [Table 1](#)). In the next step, we compared the association of TAPSE and TAPSE/PASP with effective pulmonary arterial elastance (Ea), as a lumped measure of RV afterload. Both parameters were inversely and moderately related to afterload Ea, TAPSE/PASP significantly closer than TAPSE alone ($P<0.005$) ([Table 1](#) and [Figure 1](#)).

For further clarification of this findings, we dissected out the relationship of TAPSE and its ratio to PASP with the three haemodynamic components of Ees (Ees=Piso-ESP/SV) and Ea (ESP/SV). Piso-ESP and SV slightly correlated ($r=0.3$, $P=0.01$) with each other. Both TAPSE and TAPSE/PASP showed a statistically comparable moderate association with stroke SV. However, only TAPSE significantly correlated with Piso-ESP ($r=0.45$, $P<0.001$) ([Supplementary data](#) online, [Figure S3B](#)). Regarding the afterload Ea, we detected that ESP and SV were moderately inversely associated with each other ([Supplementary data](#) online, [Figure S2](#)). The inverse association of TAPSE/PASP ratio with ESP ($r=0.78$) was significantly closer than TAPSE alone with ESP ($r=0.6$) (difference of correlation $P<0.001$). This difference was mainly based on the very tight correlation and high concordance of PASP and ESP ([Supplementary data](#) online, [Figures S4B](#)).

FAC vs. FAC/PASP

The PV loop analysis regarding FAC/PASP ratio vs. FAC is presented in [Supplementary data](#) online, [Table S3](#) and [Figure S5](#). In principle, we found very similar results, however, with one exception: the FAC alone was significantly closer associated with Ees/Ea than with FAC/PASP. Interestingly, FAC was significantly closer associated with Ees/Ea than with TAPSE ($P<0.001$).

Relevance of RV–PA coupling surrogates TAPSE and TAPSE/PASP for the prognosis

Of the 74 patients with PH, 45 (47%) died during a median follow-up of 4.8 years (2.4–6.7). Using ROC analysis to discriminate survival vs. non-survival within the observation time, we found no significant

difference ($P=0.78$) in the area under the curve (AUC) between TAPSE (AUC = 0.702, $P=0.001$) and TAPSE/PASP (AUC = 0.709, $P=0.001$) ([Figure 2A](#)). We identified cut-offs of 17 mm for TAPSE and 0.38 mm/mmHg for TAPSE/PASP to discriminate long-term survival, which was confirmed by Kaplan–Meier analysis ([Figure 2B](#)). For PASP (AUC = 0.34, $P=0.019$), we identified a prognostic cut-off of 52 mmHg. The comparison of prognostic relevance between FAC and FAC/PASP is seen in [Supplementary data](#) online, [Figure S6A](#) and B. The independent prognostic value of TAPSE and TAPSE/PASP was tested by multivariate Cox regression analysis using two different models ([Table 2](#) and [Supplementary data](#) online, [Table S5](#)). Invasive Ees/Ea, TAPSE, and TAPSE/PASP were included separately in the models because of a strong collinearity between them. Within Model 1, consisting exclusively of non-invasive parameters with univariate prognostic value both parameters, TAPSE and TAPSE/PASP showed an independent prognostic value for long-term survival. In addition, both models (Model 1: exclusively non-invasive parameter and Model 2: non-invasive and invasive parameter) were applied to the entire study cohort of 110 patients with and without PH with very similar results regarding the prognostic relevance of TAPSE and TAPSE/PASP ([Supplementary data](#) online, [Table S6](#)).

Concordance of patient groups, stratified by the cut-offs 17 mm for TAPSE and 0.38 mm/mmHg for TAPSE/PASP

The comparable prognostic significance seemed to be essentially justified by the high correlation between TAPSE and TAPSE/PASP ($r=0.92$, $P<0.001$). In addition, we found a high match of the patient groups stratified by TAPSE ≥ 17 mm and TAPSE/PASP ≥ 0.38 mm/mmHg and vice versa between patients with TAPSE < 17 mm and TAPSE/PASP < 0.38 mm/mmHg ([Figure 3](#) and [Supplementary data](#) online, [Figure S7](#)). In addition, they are concentrated below the prognostically relevant PASP cut-off of 52 mmHg in 80% of the cases.

Discussion

The exact quantification of RV–PA coupling is complex because it needs a measure that accounts for both intrinsic RV contractility and RV pulsatile and non-pulsatile afterload simultaneously.¹³ This could be achieved using the technically demanding and invasive PV catheter technique. Therefore, more easily obtainable and simple non- or semi-invasive surrogates are being sought. Guazzi et al.⁶ proposed the use of the TAPSE/PASP ratio as a straightforward and non-invasive surrogate of the invasive RV–PA coupling ratio Ees/Ea. By applying TAPSE/PASP to the concept of invasive RV–PA coupling, TAPSE would represent the invasive RV contractility Ees and PASP the afterload (Ea). In our study, PASP correlated moderately with highly with invasive Ea ($r=0.74$, $P<0.001$) and, therefore, also represented, at least partly, RV afterload. TAPSE correlated only slightly with Ees and was simultaneously inversely related to afterload Ea or PASP. However, a reflection of RV contractility increase (homeometric regulation) to increasing afterloads by TAPSE would require a positive correlation between the latter and Ea or PASP. Therefore, our data rather suggest that TAPSE does not represent contractility per se. It represents longitudinal RV deformation affected by intrinsic contractility, pulsatile, and non-pulsatile afterload. Indeed, the very

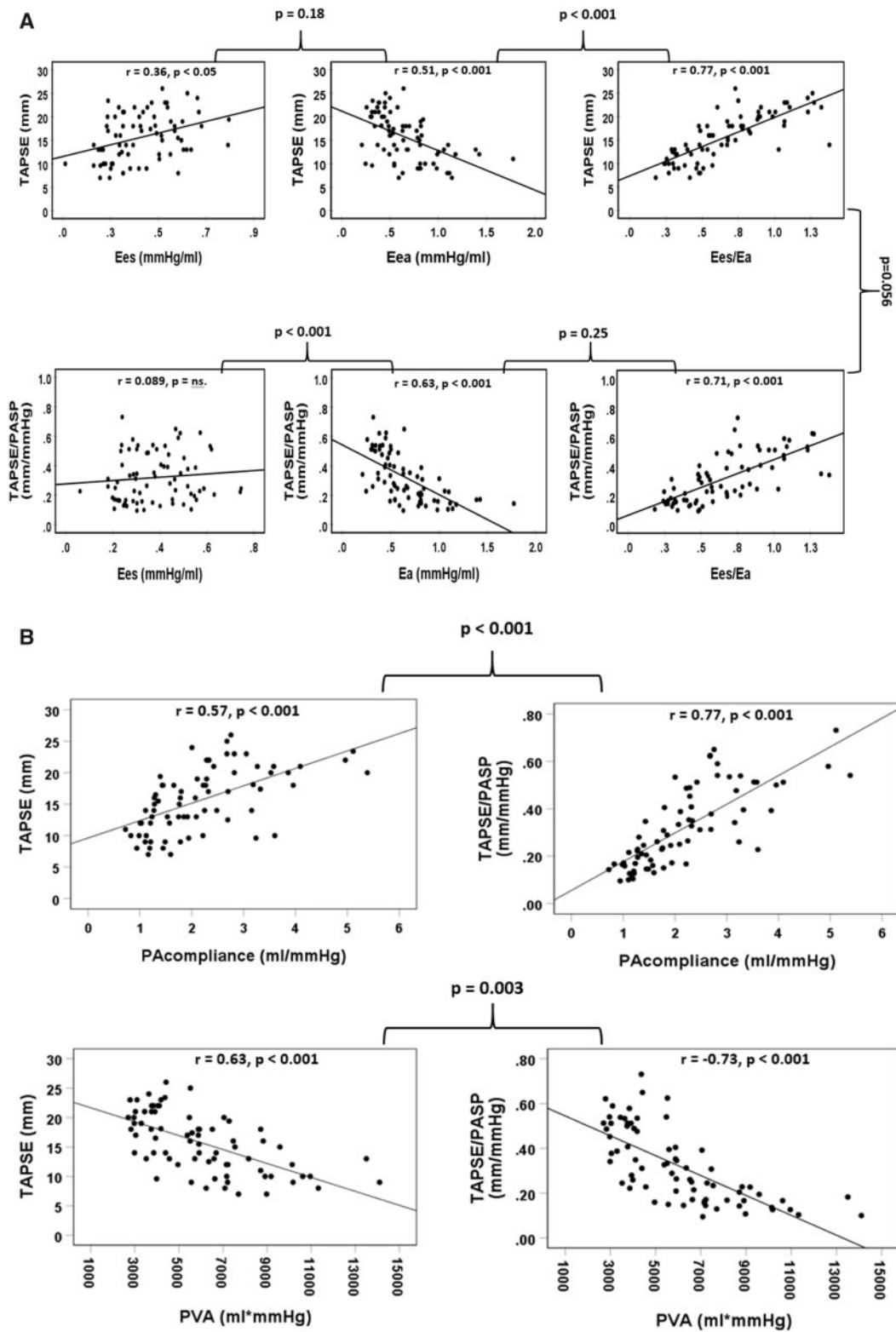


Figure 1 Relationships of (A) pressure–volume loop-derived Ees, Ea, and Ees/Ea with TAPSE and TAPSE/PASP ratio in PH patients and (B) TAPSE and TAPSE/PASP with PA compliance and PV area as surrogate for RV oxygen consumption. Solid lines represent the regression lines with Spearman correlation coefficients. The *P* values outside the graphics denote calculated statistical difference between two correlation coefficients.¹⁴ Ea, pulmonary arterial elastance; Ees, right ventricular end-systolic elastance; PA, pulmonary artery; PASP, pulmonary arterial systolic pressure; PV, pressure–volume; RV, right ventricular; TAPSE, tricuspid annular plane systolic excursion.

Table 1 Correlation analysis of non-invasive echocardiographic indices TAPSE and TAPSE/PASP with invasive PV loop and right heart catheter-derived parameter of RV volumes, contractility, diastolic function, afterload, and coupling in patients with HFREF and secondary PH (PA mean ≥ 25 mmHg) (N = 74)

	TAPSE/PASP <i>r</i>	TAPSE <i>r</i>	TAPSE/PASP vs. TAPSE (<i>P</i>)
RV-PA coupling			
Ees/Ea	0.71**	0.77**	0.056
SV/ESV	0.63**	0.61**	0.6
RV contractility			
Ees	0.089	0.36*	<0.001
Piso-PES	0.19	0.45**	<0.001
RV diastolic function			
RA mean	-0.53**	-0.41**	0.005
dp/dt _{min}	0.50**	0.28*	<0.001
RV volumes/work			
RV-EDV	-0.59**	-0.60**	0.78
RV-ESV	-0.68**	-0.67**	0.76
stroke volume (forward)	0.56**	0.55**	0.79
Stroke work (total)	-0.59**	-0.44**	<0.001
Pulmonary afterload			
Eea	-0.63**	-0.51**	0.005
ESP	-0.78**	-0.6**	<0.001
PVR	-0.49**	-0.41**	0.06
PA-CA	0.77**	0.57**	<0.001
PCWP	-0.58**	-0.36*	<0.001
DPD	0.06	-0.01	na.
TPG	-0.44**	-0.31*	0.003
RV energetics			
PVA (ln)	-0.73**	-0.63**	0.003
ME	0.65**	0.72**	0.04
LV function			
LV-EF	0.18	0.24*	0.2

DPD, diastolic pressure gradient; Ea, pulmonary arterial elastance; Ees, right ventricular end-systolic elastance; Piso, maximum pressure of isovolemic RV beat; ESP, P-endsystolic; LV-EF, left ventricular ejection fraction; ME, mechanical efficiency; PA-CA, pulmonary arterial compliance; P, pressure; PASP= systolic pulmonary arterial pressure; PCWP, pulmonary capillary wedge pressure; PVA, pressure volume area; PVR, pulmonary vascular resistance; *r*, correlation coefficient; RA, right atrial; RV-EDV, RV-end-diastolic volume; RV-ESV, RV-end-systolic volume; TAPSE, tricuspid annular plane systolic excursion; TPG, transpulmonary pressure gradient.

*Significance of correlation analysis $P < 0.05$.

**Significance of correlation analysis $P \leq 0.001$.

close relationship of TAPSE with invasive Ees/Ea ($r = 0.77$, $P < 0.001$) in our study, which was significantly closer than its correlation with Ees and with the inverse association with the afterload EA, supports our hypothesis that TAPSE itself is a surrogate of the RV-PA coupling process. Consequently, we observed that other RV parameters affected by the RV-PA coupling efficiency such as RV end-diastolic/systolic dimensions, the SV, and the occurrence of a significant tricuspid regurgitation (TR2/3)⁹ were also significant associated with TAPSE.

Interestingly, putting TAPSE into ratio with PASP did not further improve the coupling information ($r = 0.71$). On the contrary, TAPSE/PASP ratio seems to reduce the relationship to invasive Ees/Ea rather than strengthening it (difference of correlations of TAPSE and TAPSE/PASP with Ees/Ea $P = 0.056$). Validating data on FAC alone and its ratio with PASP further supports this finding. Indeed, putting FAC in ratio with PASP lowered the association to PV loop Ees/Ea in comparison to FAC alone or Ees/Ea. In addition, TAPSE/

PASP (and FAC/PASP, as well) did not correlate with Ees, and the association between TAPSE/PASP and the coupling ratio Ees/Ea was not statistically closer than its inverse relationship with the afterload Ea. The latter is interesting because TAPSE/PASP was significantly more related to global afterload (Ea) than TAPSE alone. The PV loop-derived Ea is defined by the ratio of ESP and SV. The closer relationship of TAPSE/PASP ratio with Ea is based on its significant higher inverse correlation with PV loop-derived ESP and the comparable association of both TAPSE and TAPSE/PASP with forward SV (Supplementary data online, figures and Table 1). The ESP values, in turn, highly correlated and showed a high concordance with PASP in our secondary PH patients (correlation and Bland-Altman analysis, Supplementary data online, Figure S4B), a fact previously shown in patients with pre-capillary PH, as well.¹⁶ ESP, in turn is a crucial parameter for calculation of stroke work and consecutively PVA, as a lumped measure of RV oxygen consumption, and is additionally inversely associated with diastolic RV function. Thus, concordance of

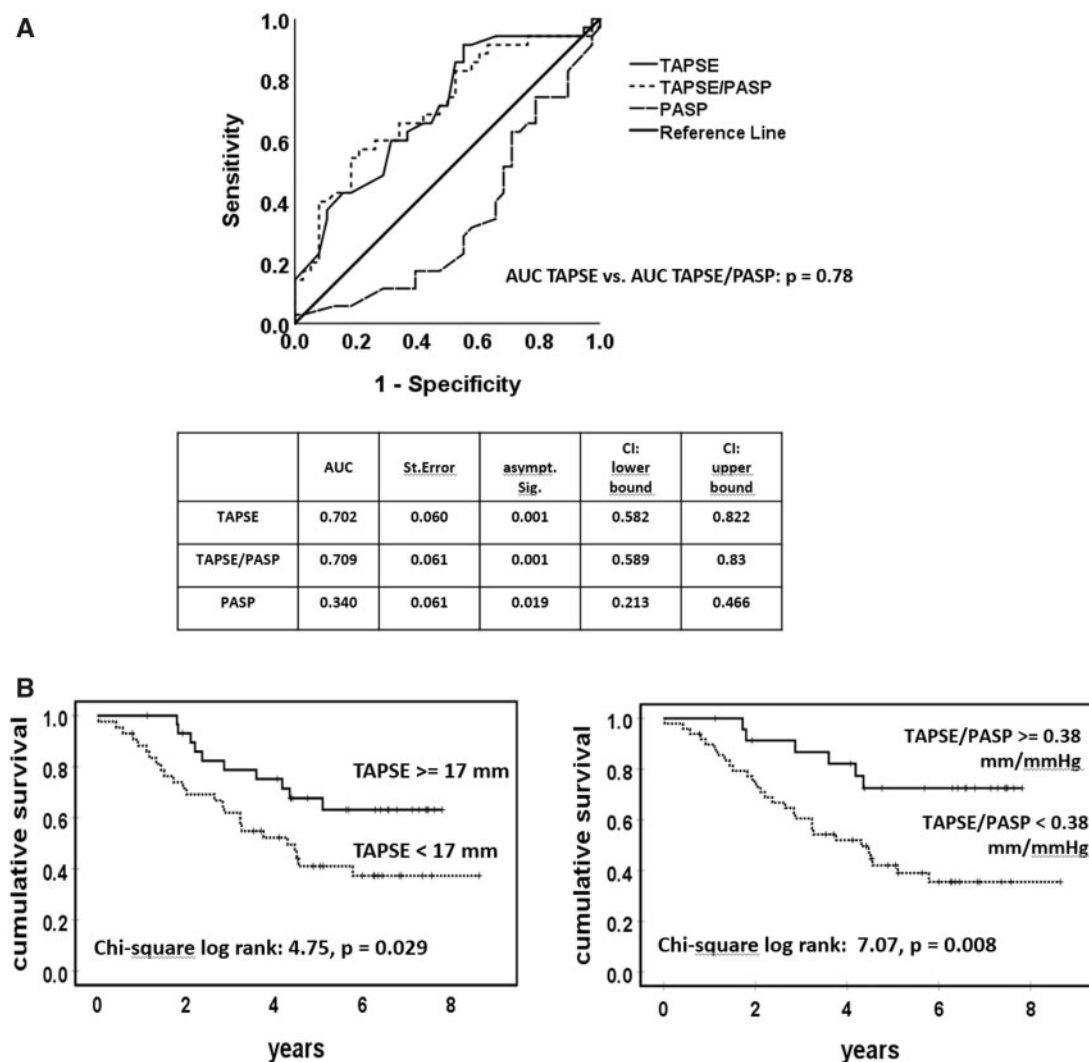


Figure 2 Receiver operating characteristic (ROC) analysis and Kaplan–Meier plots of outcome. (A) The ROC analysis of TAPSE, TAPSE/PASP, and PASP for discriminating all-cause mortality and long-term survival (mean FU 4.8 years). All parameters were evaluated together in one ROC model. (B) Kaplan–Meier plots of outcome in patients stratified by TAPSE and TAPSE/PASP. Stratification by echocardiographic TAPSE (<17 and ≥ 17 mm) (left) revealed significant differences in overall survival. Right: TAPSE/PASP (<0.38 and ≥ 0.38 mm/mmHg) with significant overall survival difference. AUC, area under the curve; PASP, pulmonary arterial systolic pressure; TAPSE, tricuspid annular plane systolic excursion.

ESP and PASP will inevitably lead to a closer relationship of diastolic dysfunction and oxygen consumption of the RV with the TAPSE/PASP ratio, than with TAPSE alone. Furthermore, PASP is sensitive to pulsatile loading effects, such as wave reflection, which will increase the association of the TAPSE/PASP ratio with Swan-Ganz-derived PA-compliance as a lumped parameter of pulsatile loading.

In principle, our analysis regarding the relationship of TAPSE/PASP with the invasive PV loop measurements confirms previously published data by Tello *et al.*,⁷ which were obtained from patients with pre-capillary PH (chronic thromboembolic PH and pulmonary arterial hypertension). They found no correlation between TAPSE/PASP and RV contractility E_{es} , a moderately inverse relationship to the afterload E_a , and a similar moderate, but positive correlation with E_{es}/E_a . In contrast to Tello *et al.*,⁷ our data imply that TAPSE as a

single parameter is already the result of the contractility adaptation to the afterload and, consequently, a suitable and straightforward surrogate parameter for RV–PA coupling in patients with HFREF (Supplementary data online, Table S4) and especially for the subgroup of patients with secondary PH. Interesting findings were previously published albeit with focus on heart failure with preserved EF (HFPEF). Guazzi *et al.*¹⁷ showed similar findings regarding the close relationship of TAPSE/PASP and pulsatile load (PA-compliance) but only a relatively limited correlation between TAPSE/PASP and the invasive (Swan-Ganz) RV–PA coupling ratio E_{es}/E_a ($r = 0.35$, $P < 0.001$). However, calculation of E_{es} by a ratio of PASP/RV end-systolic area seemed not an appropriate and validated measure for load-independent RV contractility in this study. In addition, TAPSE/PASP was associated with systolic/diastolic LV dysfunction, RV

Table 2 Stepwise multivariate cox regression analysis for all-cause mortality in patients with PH (n = 74)

Model 1			
Variables separately included into the Model 2	Independent predictors	HR (95% CI)	P
A: TAPSE	TAPSE	0.92 (0.85–0.99)	0.046
	RV-SV	0.97 (0.94–0.99)	0.037
B: TAPSE/PASP	TAPSE/PASP	0.07 (0.005–0.920)	0.043
	RV-SV	0.97 (0.94–0.99)	0.039

Model including exclusively non-invasive parameters: the parameters with univariate significance for all-cause mortality which were included within the model are severity of tricuspid regurgitation (TR), severity of mitral regurgitation (MR), end-systolic area of RV within the four-chamber view (ESA-4chv), echocardiographic-derived right ventricular forward stroke volume (RV-SV) and right atrial area (RAae). The echo-derived A: TAPSE, and B: TAPSE/PASP were separately included within the model. A joint analysis of both parameters within the model was not applicable because of a strong collinearity between them. PASP, pulmonary arterial systolic pressure; RV, right ventricular; SV, stroke volume; TAPSE, tricuspid annular plane systolic excursion.

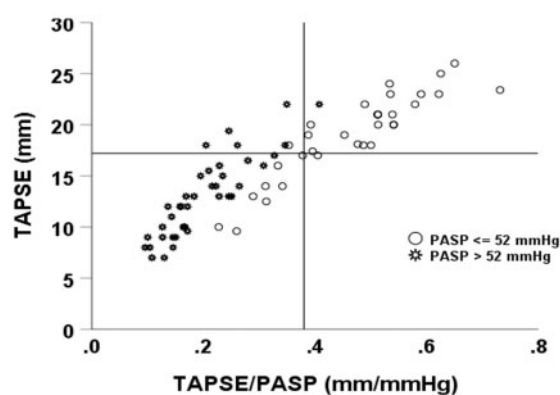


Figure 3 Concordance of patients groups stratified according their prognostic relevance. Scatterplot of relationship of TAPSE with TAPSE/PASP, stratified by PASP ≥ 52 vs. < 52 mmHg. The vertical line denotes the prognostic relevant cut-off of 0.38 mm/mmHg for TAPSE/PASP. The horizontal line denotes the prognostic relevant cut-off of 17 mm for TAPSE. PASP, pulmonary arterial systolic pressure; TAPSE, tricuspid annular plane systolic excursion.

dilatation, PH, and prognosis. However, the role of TAPSE alone was not analysed in this study. In a *post hoc* analysis of the RELAX trial,¹⁸ it was shown that TAPSE/PASP better correlated with signs of more advanced HFPEF including the severity of LV diastolic dysfunction and increased biomarker levels such as NT-pro-BNP and endothelin. However, the peak oxygen consumption (% predicted VO_2) and the ventilatory inefficiency (VE/CO_2), which were associated with the severity of RV dysfunction, similarly correlated with TAPSE and TAPSE/PASP, respectively. However, this study did not include a comprehensive invasive and echocardiographic comparative analysis of TAPSE and TAPSE/PASP regarding the relationship to pulmonary vascular load, RV dimension and function, or prognosis.

Against this background, we compared the prognostic relevance of TAPSE and TAPSE/PASP. Using ROC analysis to discriminate survival vs. non-survival within the mean observation time of 4.8 years, we found no significant difference in the AUC between TAPSE and

TAPSE/PASP. The best cut-offs to discriminate long-term survivors within the Kaplan–Meier analysis were 0.38 mm/mmHg for TAPSE/PASP and 17 mm for TAPSE, which are within the range previously associated with survival in heart failure patients.⁶ In addition, within multivariate Cox regression analysis, both TAPSE and TAPSE/PASP remained independently predictive for long-term survival in patients with HFREF and within the subgroup of patients with secondary PH, at least when using a model that included only non-invasive parameters. Our survival data confirm other data focusing on the interaction of RV functional parameters and survival in patients with secondary PH due to heart failure. A systematic review and meta-analysis concentrating exclusively on HFPEF patients could show that RV dysfunction and PH, defined by a TAPSE < 16 mm and PASP ≥ 35 mmHg or PAm_{mean} ≥ 25 mmHg are both associated with poor outcome.¹⁹ The analysis of TAPSE/PASP ratio was not included in this study. In contrast, Ghio et al.²⁰ demonstrated that TAPSE and TAPSE/PASP were both independent predictors of poor prognosis in patients with HFREF.

The apparently comparable prognostic significance of TAPSE and TAPSE/PASP in our patient population seems to be caused by a very high correlation between both parameters ($r = 0.9$) with a high match of both the prognostic favourable and the unfavourable stratified patient groups. Patients stratified by the prognostically advantageous TAPSE ≥ 17 mm, for instance, were simultaneously associated with the prognostic favourable TAPSE/PASP ≥ 0.38 mm/mmHg in 77% of the cases and are mainly (80%) concentrated below the prognostic relevant PASP cut-off of 52 mmHg. By contrast, patients stratified by the TAPSE/PASP ≥ 0.38 mm/mmHg consisted almost exclusively of patients with a TAPSE ≥ 17 mm and a PASP < 52 mmHg (96%). This indicates that stratifying patients according to the TAPSE/PASP ≥ 0.38 mm/mmHg would narrow the entire favourably coupled group (TAPSE ≥ 17 mm) down to favourably coupled patients with a low and prognostically favourable PASP < 52 mmHg. Indeed, the invasively measured PAm_{mean} values of 28 ± 3 mmHg were only slightly increased within this low-risk group.

When comparing TAPSE and TAPSE/PASP regarding the clinical usability, it should also not be neglected that the echocardiographic calculation of PASP for the TAPSE/PASP ratio needs an adequate TR velocity signal, which is not always present. In a previously published database of 1262 patients with transthoracic echocardiography who

were referred for right heart catheterization, 36% had no reported TR velocity.²¹ In addition, in our analysis we found that FAC, as a measure combining radial and longitudinal RV contraction, seemed to be a better coupling parameter than TAPSE, which reflects exclusively longitudinal deformation. However, because of the known limitations of a correct echocardiographic FAC determination, TAPSE appears more useful in daily clinical practice for RV–PA coupling analysis.

For other reasons, it seems reasonable to determine the PASP together with TAPSE or FAC, but not as ratio, if an adequate TR velocity signal is present. The height of PASP at which RV function is impaired (uncoupled) can indicate the cause of the uncoupling. A significantly lowered TAPSE (or FAC) in relationship with normal, only small or moderately increased PASP values especially may indicate an additional intrinsic injury/involvement of the RV within the left heart disease. However, in association with strong increases in PASP, an uncoupled RV may, at least partly or completely, be explained by its afterload sensitivity due to the specific anatomy and the absence of sufficient contractile muscle mass of an otherwise healthy right heart. Indeed, the afterload sensitivity of the RV–PA coupling was demonstrated in our patients with HFREF with and without secondary PH by an inverse correlation of the invasive Ees/Ea with PASP (Supplementary data online, Figure S4A). TAPSE as a surrogate of RV coupling showed the same behaviour and decreases with higher afterloads (additional data Figure 4B).

Limitations

Our study has several limitations. This is a *post hoc* analysis of a single-centre, prospective observational study of a relatively small patient group. Despite the known accuracy of echocardiographically determined TAPSE/PASP,⁶ an adequate TR velocity was not measurable in seven patients with PH (9%) and in nine patients without PH (25%). This fact would have further reduced the analysable patient group. Therefore, we determined PASP invasively by the Swan-Ganz method to compare TAPSE with TAPSE/PASP.

Similar to Tello *et al.*,⁷ the SB method was used to estimate Ees and Ea without validation against the multi-beat approach. The latter more invasive approach requires generation of multiple PV loops while varying the RV preload. This is achieved by quick occlusion of the inferior vena cava with an inflated balloon. However, we found that in patients with HFREF, ~30–40% of the balloon inflations did not lead to a significant reduction in the RV preload.

Conclusion

TAPSE is an easily and reliably obtainable and valid surrogate parameter for the RV adaption process to afterload (RV–PA coupling) in secondary PH due to HFREF. Combining TAPSE with PASP as a ratio improved information neither on RV–PA coupling nor on prognosis. On the contrary, especially in secondary PH due to HFREF, TAPSE/PASP could even obscure RV contractile dysfunction and/or RV load because both numerator and denominator are simultaneously affected. In addition, calculation of non-invasive PASP needs an adequate TR velocity signal, which is not always present. Therefore, TAPSE seems more useful in clinical practice for RV–PA coupling

analysis than its ratio with PASP. However, more prospective studies with more patients are needed to evaluate the additive value of TAPSE/PASP vs. TAPSE alone in clinical risk assessment and subsequent therapeutic strategy for HFREF patients with secondary PH.

Supplementary data

Supplementary data are available at *European Heart Journal - Cardiovascular Imaging* online.

Funding

This study was supported by a grant from Boston Scientific.

Conflict of interest: There is no conflict of interest.

Data availability

The data underlying this article are available in the article and in its online supplementary material.

References

- Naeije R, Brimiouille S, Dewachter L. Biomechanics of the right ventricle in health and disease (2013 Grover Conference series). *Pulm Circ* 2014;**4**:395–406.
- Sagawa K. The end-systolic pressure-volume relation of the ventricle: definition, modifications and clinical use. *Circulation* 1981;**63**:1223–7.
- Maughan WL, Shoukas AA, Sagawa K, Weisfeldt ML. Instantaneous pressure-volume relationship of the canine right ventricle. *Circ Res* 1979;**44**:309–15.
- Sunagawa K, Maughan WL, Burkhoff D, Sagawa K. Left ventricular interaction with arterial load studied in isolated canine ventricle. *Am J Physiol* 1983;**245**:H773–80.
- Hsu S. Coupling right ventricular-pulmonary arterial research to the pulmonary hypertension patient bedside. *Circ Heart Fail* 2019;**12**:e005715.
- Guazzi M, Bandera F, Pelissero G, Castelvécchio S, Menicanti L, Ghio S *et al.* Tricuspid annular plane systolic excursion and pulmonary arterial systolic pressure relationship in heart failure: an index of right ventricular contractile function and prognosis. *Am J Physiol Heart Circ Physiol* 2013;**305**:H1373–81.
- Tello K, Wan J, Dalmer A, Vanderpool R, Ghofrani HA, Naeije R *et al.* Validation of the Tricuspid Annular Plane Systolic Excursion/Systolic Pulmonary Artery Pressure Ratio for the Assessment of Right Ventricular-Arterial Coupling in Severe Pulmonary Hypertension. *Circ Cardiovasc Imaging* 2019;**12**:e009047.
- Santamore WP, Dell'Italia LJ. Ventricular interdependence: significant left ventricular contributions to right ventricular systolic function. *Prog Cardiovasc Dis* 1998;**40**:289–308.
- Schmeisser A, Rauwolf T, Ghanem A, Groscheck T, Adolf D, Grothues F *et al.* Right heart function interacts with left ventricular remodeling after CRT: a pressure-volume loop study. *Int J Cardiol* 2018;**268**:156–61.
- Lang RM, Badano LP, Mor-Avi V, Afilalo J, Armstrong A, Ernande L *et al.* Recommendations for cardiac chamber quantification by echocardiography in adults: an update from the American Society of Echocardiography and the European Association of Cardiovascular Imaging. *J Am Soc Echocardiogr* 2015;**28**:1–39.
- Zoghbi WA, Adams D, Bonow RO, Enriquez-Sarano M, Foster E, Grayburn PA *et al.* Recommendations for noninvasive evaluation of native valvular regurgitation: a report from the American Society of Echocardiography Developed in Collaboration with the Society for Cardiovascular Magnetic Resonance. *J Am Soc Echocardiogr* 2017;**30**:303–71.
- Rosenkranz S, Diller GP, Dumitrescu D, Ewert R, Ghofrani HA, Grunig E *et al.* Hemodynamic definition of pulmonary hypertension: commentary on the Proposed Change by the 6th World Symposium on Pulmonary Hypertension. *Dtsch Med Wochenschr* 2019;**144**:1367–72.
- Ten Brinke EA, Klautz RJ, Verwey HF, van der Wall EE, Dion RA, Steendijk P. Single-beat estimation of the left ventricular end-systolic pressure-volume relationship in patients with heart failure. *Acta Physiol (Oxf)* 2010;**198**:37–46.
- Rosner B, Wang W, Eliassen H, Hibert E. Comparison of dependent Pearson and Spearman correlation coefficients with and without correction for measurement error. *J Biom Biostat* 2015;**6**:2–9.
- DeLong ER, DeLong DM, Clarke-Pearson DL. Comparing the areas under two or more correlated receiver operating characteristic curves: a nonparametric approach. *Biometrics* 1988;**44**:837–45.


16. Tello K, Richter MJ, Axmann J, Buhmann M, Seeger W, Naeije R et al. More on single-beat estimation of right ventriculoarterial coupling in pulmonary arterial hypertension. *Am J Respir Crit Care Med* 2018;**198**:816–8.
17. Guazzi M, Dixon D, Labate V, Beussink-Nelson L, Bandera F, Cuttica MJ et al. RV contractile function and its coupling to pulmonary circulation in heart failure with preserved ejection fraction: stratification of clinical phenotypes and outcomes. *JACC Cardiovasc Imaging* 2017;**10**:1211–21.
18. Hussain I, Mohammed SF, Forfia PR, Lewis GD, Borlaug BA, Gallup DS et al. Impaired right ventricular-pulmonary arterial coupling and effect of sildenafil in heart failure with preserved ejection fraction: an ancillary analysis from the phosphodiesterase-5 inhibition to improve clinical status and exercise capacity in diastolic heart failure (RELAX) trial. *Circ Heart Fail* 2016;**9**:e002729.
19. Gorter TM, Hoendermis ES, van Veldhuisen DJ, Voors AA, Lam CS, Geelhoed B et al. Right ventricular dysfunction in heart failure with preserved ejection fraction: a systematic review and meta-analysis. *Eur J Heart Fail* 2016;**18**:1472–87.
20. Ghio S, Guazzi M, Scardovi AB, Klersy C, Clemenza F, Carluccio E, on behalf of all investigators et al. Different correlates but similar prognostic implications for right ventricular dysfunction in heart failure patients with reduced or preserved ejection fraction. *Eur J Heart Fail* 2017;**19**:873–9.
21. O'Leary JM, Assad TR, Xu M, Farber-Eger E, Wells QS, Hemnes AR et al. Lack of a tricuspid regurgitation Doppler signal and pulmonary hypertension by invasive measurement. *J Am Heart Assoc* 2018;**7**:e009362.

IMAGE FOCUS

doi:10.1093/ehjci/jeaa161

Online publish-ahead-of-print 12 June 2020

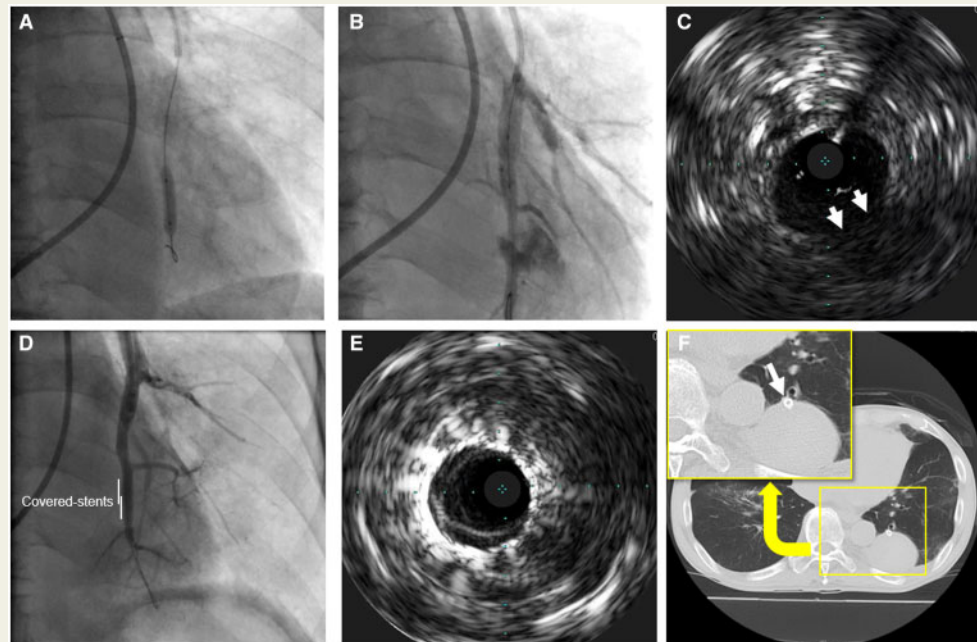
Angiographic and intravascular ultrasound images of pulmonary artery rupture during balloon pulmonary angioplasty

Kazuhiko Nakazato *, Koichi Sugimoto, Takatoyo Kiko, Atsushi Kobayashi, and Yasuchika Takeishi

Department of Cardiovascular Medicine, Fukushima Medical University, 1, Hikariga-oka, Fukushima-shi, Fukushima 960-1295, Japan

* Corresponding author. Tel: +81 24 547 1190; Fax: +81 24 548 1821. E-mail: nakazato@fmu.ac.jp

A 75-year-old man who was diagnosed with inoperable chronic thromboembolic pulmonary hypertension underwent balloon pulmonary angioplasty (BPA) in his right lower lobe pulmonary artery (Panel A). Soon after the ballooning, rupture of the pulmonary artery occurred (Panel B and [Supplementary data online, Video S1](#)). We urgently observed the lesion with intravascular ultrasound (IVUS) and recognized that part of the vessel wall structure had disappeared (allows in Panel C and [Supplementary data online, Video S2](#)). After



IVUS observation, we rapidly placed two covered-stents (JOSTENT GraftMaster, Abbott Vascular, Santa Clara, CA, USA) to stop bleeding, and pulmonary angiography revealed the disappearance of extravasation of contrast medium (Panel D and [Supplementary data online, Video S3](#)). In IVUS observation, the ruptured lesion was repaired with covered-stents (Panel E and [Supplementary data online, Video S4](#)). Chest computed tomography taken 30 days after BPA showed encapsulated pulmonary haemorrhage and a high-density image of covered-stents in the right lower lobe (white allow in Panel F). Unlike guidewire perforation, the IVUS images demonstrated that the vessel wall structure was partially lost. In such a case, treatment with a covered-stent may be the only way to bail out of a nightmare. Although there have been a few reports of treating pulmonary artery rupture with covered-stents, to our best knowledge, this is the first report to show IVUS images of ruptured pulmonary artery during BPA.

[Supplementary data](#) are available at *European Heart Journal - Cardiovascular Imaging* online.

© The Author(s) 2020. Published by Oxford University Press on behalf of the European Society of Cardiology.

This is an Open Access article distributed under the terms of the Creative Commons Attribution Non-Commercial License (<http://creativecommons.org/licenses/by-nc/4.0/>), which permits non-commercial re-use, distribution, and reproduction in any medium, provided the original work is properly cited. For commercial re-use, please contact journals.permissions@oup.com